Mon. Not. R. Astron. Soc. **000**, 000–000 (0000) Printed 23 September 2009 (MN LATEX style file v2.2)

Galaxy Number Counts and Implications for Strong Lensing

C. D. Fassnacht,[1], L. V. E. Koopmans,[2] and K.C. Wong[1,3]
[1]*Department of Physics, University of California Davis, 1 Shields Avenue, Davis, CA 95616, USA*
[2]*Kapteyn Astronomical Institute, P.O. Box 800, 9700 AV Groningen, Netherlands*
[3]*Current Address: Astronomy Department/Steward Observatory, University of Arizona, 933 N. Cherry Ave., Tucson, AZ 85721, USA*

23 September 2009

ABSTRACT
We compare galaxy number counts in Advanced Camera for Surveys (ACS) fields containing moderate-redshift ($0.2 < z < 1.0$) strong gravitational lenses with those in two comparison samples: (1) the first square degree of the COSMOS survey, comprising 259 ACS fields and (2) 20 "pure parallel" fields randomly located on the sky. Through a Bayesian analysis we determine the expectation values (μ_0) and confidence levels of the underlying number counts for a range of apertures and magnitude bins. Our analysis has produced the following results: (i) We infer that our control samples are not consistent at the >10–σ level, with the number counts in the COSMOS sample being higher than in the pure parallel sample. This result matches those found in previous analyses of COSMOS data using different techniques. (ii) We find that small-size apertures, centered on strong lenses, are overdense around the 2–σ level compared with randomly placed apertures in the control samples, even compared to the COSMOS sample. Correcting for the local clustering of elliptical galaxies, based on the average two-point correlation function, this over density reduces to the $\lesssim$1–σ level. Thus, the overdensity of galaxies seen *along* a typical line of sight to a lens can be explained by the natural clustering of galaxies, rather than being due to lenses lying along otherwise biased lines of sight. (iii) Despite the considerable scatter in the lines of sight to *individual* lens systems, we find that quantities that are linearly dependent on the external convergence (e.g. H_0) should become unbiased if the few extra galaxies that cause the bias (i.e. $\Delta\mu_0 \lesssim 2.0$ galaxies with $19 \leq m \leq 24$ for aperture sizes $\leq 45''$ radius) can be accounted for in the lens models.

Key words: gravitational lensing – large-scale structure of Universe – distance scale

1 INTRODUCTION

Strong gravitational lenses, where multiple images of the background object are formed, are powerful probes of the distribution of mass in the Universe. The properties of the lensed images are, in principle, sensitive only to the projected mass of the lensing object, with no requirements that the mass be luminous or baryonic (e.g., Schneider, Kochanek, & Wambsganss 2006). Most of the lensing signal comes from the primary lensing object – typically a massive early-type galaxy – and, if the lensing object is a member of a galaxy cluster or group, its immediate environment.

However, the distribution of large-scale structure (LSS) along the line of sight to the lens system adds perturbations to the lensing properties. For example, simulations have shown that a non-negligible fraction of lenses can only be produced by having multiple lens planes along the line of sight (Wambsganss, Bode, & Ostriker 2005; Hilbert et al. 2007, 2008). Furthermore, the differences in light travel times along rays forming the multiple lensed images in a given system can be affected at the level of a few percent (e.g., Seljak 1994) or up to $\sim$10% (e.g., Bar-Kana 1996) by the distribution of LSS along that particular line of sight. These effects should be random for random lines of sight, so it should be possible to reduce the LSS uncertainties and exploit the power of gravitational lenses as cosmological tools by averaging over many systems. If, however, lenses lie along biased lines of sight, this reduction will not occur and global parameters such as H_0 determined from large lens samples will be biased.

To date, most observational investigations of the effects of the environment on strong lensing have focused on the local neighborhood of the lens by searching for spectroscopic evidence of galaxy groups and clusters that are physically associated with the lensing galaxy (e.g., Kundić et al. 1997a,b; Fassnacht & Lubin 2002; Momcheva et al. 2006; Fassnacht et al. 2006b; Auger et al. 2007, 2008). Some of these investigations (e.g., Fassnacht & Lubin 2002; Momcheva et al. 2006; Fassnacht et al. 2006b; Auger et al. 2007) have also found mass concentrations along the line of sight that are at different redshifts than the lensing galaxy. However, due to the limitations imposed by requiring spectroscopic redshifts for their analyses, the spectroscopic surveys are necessarily incomplete samples of the line of sight. Most also are also biased because they preferentially target galaxies expected to be at the redshift of the primary lens. There have also been photometric studies of lens fields in order to evaluate lens environments. These photometric investigations are the closest in concept to the analysis in this pa-

per. However, they focused on either group finding via detection of red sequences (Williams et al. 2006), or on describing the immediate environment of the lensing galaxy by using galaxy colors to strongly favor galaxies likely to be at the redshift of the lens (Auger 2008; Treu et al. 2009). None of these previous photometric studies evaluates the contributions by galaxies along the full line of sight.

In this paper, we investigate the question of whether lens lines of sight are biased by comparing, through Bayesian and frequentist statistics, the number counts of galaxies in fields containing gravitational lenses with those obtained from two control samples. The control samples are chosen to provide reasonable approximations to typical lines of sight through the Universe. All images were obtained with the Advanced Camera for Surveys (ACS; Ford et al. 1998, 2002) aboard the *Hubble Space Telescope* (*HST*). The underlying idea is that lines of sight that are overdense in galaxies are also overdense in mass, if the underlying redshift distributions are roughly the same. Hence by simply counting galaxies, one can make conservative statements about the lines of sight towards lens galaxies that are not highly model-dependent. We discuss the sample selection and image processing in §2, do a frequentist analysis of the samples in §3, develop and use a Bayesian framework for comparing the samples in §4, briefly describe the number counts for individual lens systems (as opposed to sample averages) in §5, and interpret the results in §6.

2 DATA REDUCTION

In this section we briefly describe the data reduction and catalogue extraction.

2.1 Sample Definition and Data Processing

The lens sample comprises 18 systems which were observed with ACS as part of the CfA-Arizona Space Telescope Lens Survey (CASTLES; GO-9744; PI Kochanek). This sample was defined by taking the full list of lenses observed with ACS as part of the CASTLES program (24 galaxies in all) and only including systems that (1) had total exposure times $\gtrsim$2000 s, (2) had no extremely bright stars in the field, and (3) had galactic latitudes of $|b| > 10$. Each system was observed through the F555W and F814W filters, but for comparison with the control data sets, we only consider the F814W data. The typical total exposure times through the F814W filter were $\sim$2000–3000 sec. Details of the observations are given in Table 1. The pipeline-processed data were obtained from the Multimission Archive at Space Telescope, and the individual exposures were combined using the *multidrizzle* package (Koekemoer et al. 2002). We also included in the lens sample deep ACS images of B0218+357 (GO-9450; PI N. Jackson) and B1608+656 (GO-10158; PI Fassnacht), with total F814W exposure times of 48,720 and 28,144 sec, respectively. For easier comparison with the rest of the lens sample we only used the data from the first four F814W exposures on the B1608+656 field, with a combined integration time of 2528 sec. The lens galaxies are at moderate redshifts, with a mean and RMS of $\mu_z = 0.55$ and $\sigma_z = 0.22$, respectively. This should be compared to the environmental investigations of Auger (2008) and Treu et al. (2009), which focused on a lower redshift sample ($z \lesssim 0.3$).

Table 1. Lens Sample

Lens System	t_{exp} (sec)	$z_{\rm lens}$
JVAS B0218+357	48720	0.68
CLASS B0445+128	5228	0.557
CLASS B0850+054	2296	0.59
CLASS B1608+656	2528	0.630
CLASS B2108+213	2304	0.365
CFRS 03.1077	2296	0.938
HE 0435-1223	1445	0.46
HE 1113-0641	1317	0.75^a
J0743+1553	2300	0.19
J0816+5003	2440	...
J1004+1229	2296	0.95
Q1131-1231	1980	0.295
SDSS 0246-0825	2288	$0.72a$
SDSS 0903+5028	2444	0.388
SDSS 0924+0219	1148	0.39
SDSS 1004+4112	2025	0.68
SDSS 1138+0314	2296	0.45
SDSS 1155+6346	1788	0.176
SDSS 1226-0006	2296	0.52
WFI 2033-4723	2085	0.66

Redshifts marked with an ^{a} are photometric redshifts. All other redshifts are spectroscopic.

2.2 Control fields

The first control sample consists of data obtained by the Cosmic Evolution Survey team (COSMOS; Scoville et al. 2007a,b). The COSMOS data consist of a mosaic of approximately two square degrees, with all of the images obtained through the F814W filter. They were obtained as part of a 510-orbit HST Treasury proposal in Cycles 12 and 13 (GO-9822; PI Scoville). Each field has a total exposure time of 2028 sec, comparable in depth to the lens fields. The data have been fully reduced by the COSMOS team (Koekemoer et al. 2007), so it was not necessary to run *multidrizzle*. Instead the 257 processed science and weight images from Cycle 12 – comprising $\sim$1 square degree – were obtained from the COSMOS ACS website hosted by the NASA/IPAC Infrared Science Archive[1].

The second control sample consists of data obtained as part of a pure parallel program to search random fields for emission line galaxies (GO-9468; PI L. Yan). This program included 28 pointings in the F814W filter, of which we used the 20 that successfully passed all of the criteria required for our image processing (hereafter referred to as the "pure parallel fields"). These pure parallel fields cover a total area of $\sim$0.06 square degrees. Although the number of pointings is much smaller than obtained with the COSMOS program, the pure parallel fields have the advantage of not being contiguous on the sky and, thus, provide an important check that the COSMOS data do not have some overall bias in the number counts due to sample variance. These data were processed by the a modified version of the pipeline developed as part of the HST Archive Galaxy Gravitational Lens Survey (Marshall et al., in prep) which is designed to produce final images aligned sufficiently well to conduct weak lensing analyses. The modification to the pipeline for the pure parallel fields was simply to change the output pixel scale from the HAGGLES standard $0\farcs03$ pix^{-1} to $0\farcs05$ pix^{-1}, in order to match the COSMOS pixel scale.

[1] http://irsa.ipac.caltech.edu/data/COSMOS/images/acs_v1.2/

2.3 Object Detection and Flagging

Object catalogs were obtained by running SExtractor (Bertin & Arnouts 1996) on each ACS image. For both the lens-field and control files, the weight maps produced by *multidrizzle* were used to improve the object detection. The magnitudes used in this paper are Vega-based $F814W$ magnitudes measured within the "AUTO" aperture computed by SExtractor. Hereafter, we will use m to designate these $F814W$ Vega magnitudes. We edited the initial catalogs to reject stars and artifacts. Because the *HST* point spread function is simply the diffraction limit of the telescope rather than depending on variable seeing, a simple star-galaxy separation can be achieved by plotting the SExtractor full width at half-maximum (FWHM) parameter versus object magnitude. The stars stand out as a narrow locus of objects all with approximately the same FWHM, up until the point where they saturate (at $m \lesssim 18 - 18.5$). For brighter stars, the locus moves to larger values of the FWHM while still remaining relatively narrow, making it easy to reject the stars. However, this star-galaxy separation method does not catch false detections due to stellar diffraction spikes and bleeding from saturated regions. Most of these objects can be still be flagged automatically because they are often highly elongated. Thus, to select real galaxies from the catalogs, we rejected all sources with: (1) FWHM$< 0\farcs13$, (2) $m < 18.5$, and (3) $(b/a) < 0.12$, where a and b are the semimajor and semiminor axes, respectively.

The COSMOS catalogs required additional flagging because the images obtained from the COSMOS ACS science archive contain bands several pixels wide along their left and right edges where cosmic rays are not properly cleaned. Simple spatial masks were sufficient to eliminate the spurious sources associated with the cosmic rays. The COSMOS images were obtained at two fixed roll angles, separated by 180° (e.g., Koekemoer et al. 2007), so that two sets of masking regions were required to flag the resulting catalogs.

2.4 Definition of apertures

We compute galaxy number counts in a set of apertures with radii of $45''/(\sqrt{2})^i$, where $i = 0, 1, 2, 3$. These aperture sizes are chosen to probe how localized any differences between the lens fields and control fields may be. The lens targets are centered on one of the ACS chips, and the $i = 0$ aperture is roughly the largest that can fit on the chip without extending over the chip gap. For apertures with $i > 3$, the numbers of galaxies detected in the apertures start to drop to unacceptably small numbers on the bright end of the luminosity functions. In the case of the lens fields, the apertures are always centered on the lensing galaxy, while for the control fields the apertures were laid down on regular grids to maximize the number of independent apertures on each field while also avoiding the chip edges and chip gap. These grids consist of 4, 9, 16, and 36 apertures per pointing for aperture radii of $45''$, $31\farcs8$, $22\farcs5$, and $15\farcs9$, respectively. Thus, for each choice of aperture size there will always be 20 lens apertures, wherease the number of control field apertures will depend on the aperture size. There will be $(257 \times n)$ COSMOS and $(20 \times n)$ pure parallel apertures, where n represents the aperture-dependent number of grid points per pointing listed above.

Figure 1 shows, as an illustration, the distribution of galaxy number counts in the COSMOS fields inside apertures of radius $45''$, with lines marking the mean number counts and the regions enclosing 68% and 95% of the data. The formal errors on the mean are very small (nearly invisible on the plot), but small number statistics significantly broaden the width of the distribution at the bright end. Furthermore, the 2000 s exposure time for each COSMOS field leads to a turnover of the number counts past $m = 24$. Thus, in the following analysis we only consider objects with $19 \leq m \leq 24$.

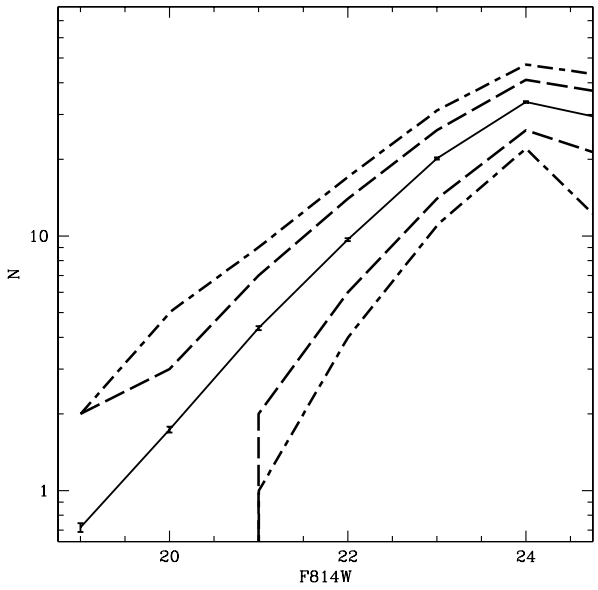

Figure 1. Number counts in the COSMOS fields, using apertures of radius $45''$. There are four such apertures per COSMOS ACS field. The thick solid line represents the mean number counts in each bin, while the negligible error bars on the line show the formal error on the mean. The dashed and dot-dashed lines enclose 68% and 90% of the data, respectively.

Of course, having the lens-field apertures chosen to be centered on the lens system introduces two sources of bias. The first is that the lens system itself contributes to the number counts in the aperture. The second bias is that lensing galaxies tend to be massive early-type galaxies and, as such, can be expected to be found in locally overdense environments (e.g., Dressler 1980; Zabludoff & Mulchaey 1998). We control the first bias by flagging the lensing galaxy and all lensed images by hand in the input catalogs. Furthermore, we exclude any galaxies within $2\farcs5$ of the lens systems to avoid any strong magnification biases associated with these bright galaxies. The correction for the second effect is discussed in §4.4. There may be some additional bias in the number counts in the lens fields due to clustering associated with the lensed background object (e.g., Fassnacht et al. 2006a), which for these systems is almost always a massive galaxy hosting an active nucleus. However, we expect this bias in the counts to appear only in the fainter magnitude bins and mostly be washed out by the large number of faint galaxies along these lines of sight.

3 FREQUENTIST ANALYSIS

In order to do an initial comparison of the three samples, we use Kolmogorov-Smirnov (KS) tests on three different pairs of samples: lens vs. COSMOS, pure-parallel vs. COSMOS, and lens vs. pure-parallel. These tests are conducted for each combination of aperture size and magnitude. Figure 2 shows examples of cumulative distributions for several combinations of aperture size and

Table 2. KS Test Results

		$\log_{10} P_{\rm KS}$		
r ($''$)	m	Lens–COSMOS	PP–COSMOS	Lens–PP
45.0	19	-0.54	-0.00	-0.40
	20	**-2.37**	-0.24	-1.89
	21	-0.84	-0.95	-0.63
	22	-0.66	**-3.22**	-0.49
	23	-0.07	**-3.78**	-0.03
	24	-0.81	-0.50	-0.61
31.8	19	-0.52	-0.00	-0.45
	20	-1.93	-0.12	-1.73
	21	-0.94	-1.69	-0.83
	22	-0.11	**-8.77**	-0.08
	23	-0.03	**-5.60**	-0.02
	24	-0.60	**-2.04**	-0.52
22.5	19	-0.09	-0.00	-0.07
	20	-0.97	-0.00	-0.90
	21	-1.23	-1.23	-1.15
	22	-0.44	**-5.64**	-0.40
	23	-0.03	-1.53	-0.02
	24	-0.50	-0.06	-0.46
15.9	19	-0.03	-0.00	-0.03
	20	-0.23	-0.00	-0.22
	21	-0.90	**-2.83**	-0.87
	22	-0.60	**-8.18**	-0.58
	23	-0.30	**-6.43**	-0.29
	24	-0.13	**-5.28**	-0.13

Results from Kolmogorov-Smirnov tests comparing pairs of samples. Values are the logarithms of the probabilities that the given pair of samples could have produced the observed D values by chance if they were drawn from the same distribution. The "PP" designation refers to the pure parallel sample. Numbers in bold are those with probabilities lower than 0.01.

magnitude bin. These plots can be used to estimate the KS D value for representative pairs of samples, as well as the sample medians. The results of the KS tests are given in Table 2, and reveal that for most of the aperture–magnitude pairs the lens fields are consistent, at greater than the 10% confidence level, with being drawn from the same distribution as the control fields; only for the comparison to the COSMOS sample in the $m = 20$ bin and the $45''$ aperture is the probability that the two samples are drawn from the same distribution less than 1%. However, the significance of any differences between the lens fields and the other samples is low due to the small number of apertures in the lens fields. With a larger sample of lens targets, the differences in distributions may become more significant.

Somewhat surprisingly, the control samples show evidence of significant difference from each other, with 10 instances where the KS test indicates that there is less than a 1% chance that the pure-parallel and COSMOS samples are drawn from the same parent distribution. Most of these low probabilities occur for the bins where $m = 22$ or 23. Furthermore, in nearly every case, it appears that the COSMOS fields are overdense compared to the pure parallel fields (e.g., Figure 2c). While this is an unexpected result, since both the COSMOS and the pure-parallel fields were chosen to be "fair" representations of the Universe, it is perfectly possible that the contiguous COSMOS area is not large enough to escape being a biased line of sight through the Universe. In fact, our results are consistent with analyses by the COSMOS team, which find that, in the magnitude range $22 < i < 23$, the field chosen for the COSMOS observations has higher clustering amplitudes than those found in surveys of other fields (McCracken et al. 2007). Also, the COSMOS weak lensing maps (Massey et al. 2007; Leauthaud et al. 2007) show more structure than seen typical simulation fields (Faure et al. 2009). In this case the pure parallel sample, albeit small, appears to provide a better indication of expected number counts in images of this depth.

4 BAYESIAN ANALYSIS

To objectively compare the number counts in the lens and control fields, and assess whether they are consistent, we also conduct a Bayesian analysis of the number count distributions.

4.1 Poisson Fluctuations

The first effect that needs to be considered in the Bayesian analysis is that of counting statistics. That is, given an underlying expectation value, μ, for the number of galaxies in a given aperture and magnitude bin, what is the likelihood function for the observed number counts, N_i, for each field i? This is simply the Poisson probability function

$$P(N_i|\mu) = \frac{e^{-\mu}\mu^{N_i}}{N_i!}, \quad (1)$$

where $P(N_i|\mu)$ is already normalized. In the top row of Figure 3 we show representative plots that include both the distributions of the observed COSMOS number counts (histograms) and the corresponding Poisson distributions with the same means (solid curves). Figure 3a shows that the Poisson description works well for distributions with small means, in this case a bright-magnitude bin for the $45''$ aperture. In contrast, as μ becomes large (e.g., Figure 3c), the observed distribution becomes wider than the predicted one, suggesting that different apertures have different underlying density fields, i.e., the same value of μ cannot be used for all apertures of a given size. Clearly the analysis requires another term.

4.2 Sample ("Cosmic") Variance

The additional term is necessary because the presence of large-scale structure produces field-to-field variations, i.e. sample variance, in the expectation value of the underlying density field. To model this large-scale structure term, commonly known as "cosmic variance" we assume that the field-to-field variations, for a fixed aperture, within the lens and control samples can, in each case, be approximated as a Gaussian random field (Bardeen et al. 1986) for $\mu > 0$, i.e.

$$P(\mu|\mu_0,\sigma_0) \propto \exp\left(-\frac{(\mu-\mu_0)^2}{2\sigma_0^2}\right) \quad (2)$$

and $P(\mu|\mu_0,\sigma_0) = 0$ for $\mu <= 0$. The integral over the probability function is properly normalized to unity. The values of μ_0 and σ_0 for a given aperture size are held fixed *within* each ensemble of fields (i.e., lens, COSMOS, or pure parallel) but can vary *between* ensembles.

Using Bayesian theory to combine the two effects gives

$$P(N_i|\mu_0,\sigma_0) = \int P(N_i|\mu)P(\mu|\mu_0,\sigma_0)d\mu, \quad (3)$$

and, combining the different fields within a given sample into a single data set $\{N_i\}$, with

$$P(\mu_0,\sigma_0|\{N_i\}) = \frac{P(\mu_0,\sigma_0)\prod_i P(N_i|\mu_0,\sigma_0)}{P(\{N_i\})}. \quad (4)$$

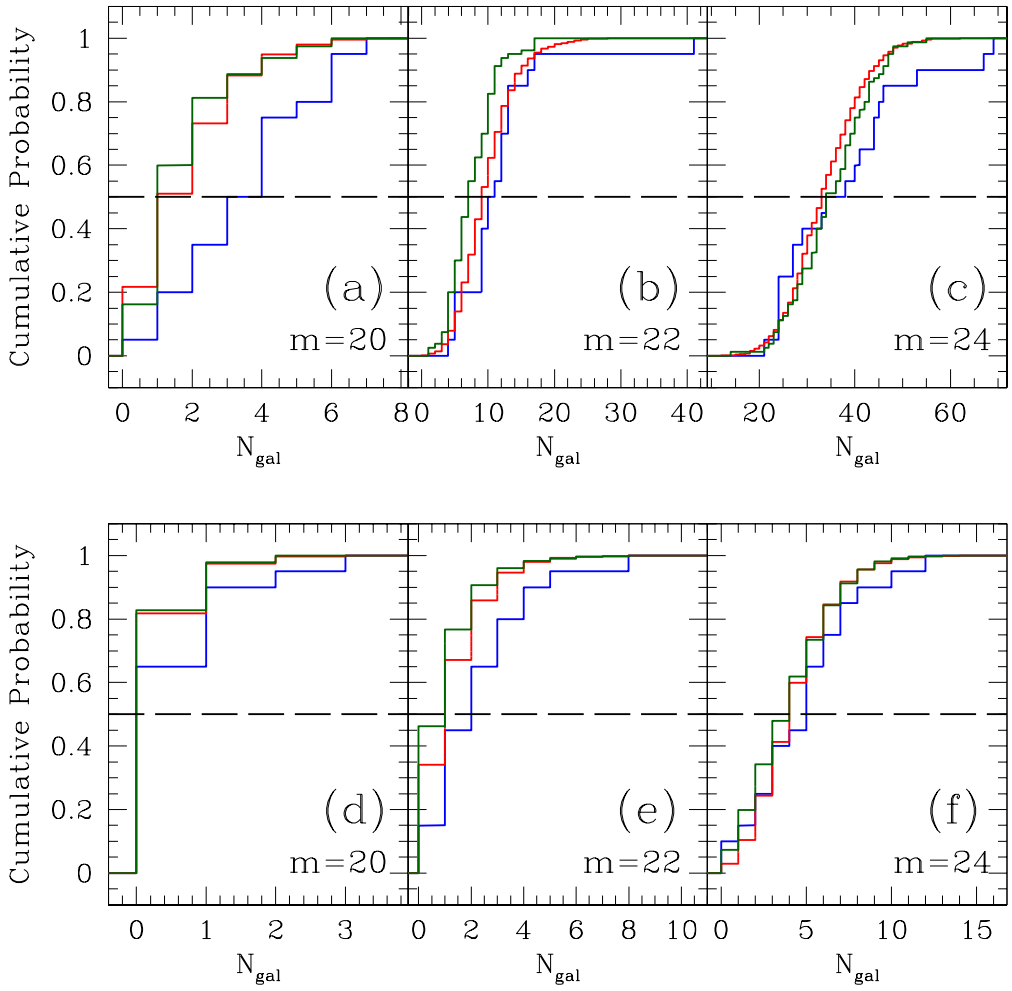

Figure 2. Cumulative distribution of number counts for six representative aperture–magnitude pairs. The top row shows apertures with radius 45″, while the bottom row shows apertures with radius 15.″9. The magnitude bin used to construct each plot is shown in the bottom right corner of the plot. The horizontal dashed line in each plot represents a cumulative probability of 0.5 and can thus be used to find the medians of the distributions. Blue curves represent the lens sample, red curves are the COSMOS sample, and green curves are the pure parallel sample.

We assume a flat prior on μ_0, because it must be invariant under shifts, and a flat prior on $\log(\sigma_0)$, because it must be invariant under multiplication (e.g., Gregory 2005). Finally, we marginalize over σ_0, which to us is a nuisance parameter, and get

$$P(\mu_0|\{N_i\}) = \int P(\mu_0, \sigma_0|\{N_i\}) d\sigma_0. \quad (5)$$

To obtain the median and 68% confidence contour, we construct a marginalized probability distribution from $P(\mu_0|\{N_i\})$ and find the μ_0 values corresponding to cumulative probabilities of 0.16, 0.5 (median), and 0.84. In Fig. 4, we illustrate the above process by an example for the 45″ aperture and for $m = 22$.

4.3 Results of Bayesian Analysis

We calculate μ_0 (i.e., the most likely average number density of galaxies) for the lens and control fields as a function of the aperture size and magnitude. The results are shown in Figure 5 and listed in Table 3.

Figure 5 shows significant differences between the values of μ_0 obtained for the two control samples. Especially in the magnitude bins corresponding to $21 \leq m \leq 23$, the COSMOS galaxy densities are systematically higher than those seen in the pure parallel fields. This result is similar to that obtained from the KS analysis (Table 2 and Figure 2) and also with the analysis by the COSMOS team, which finds that the amount of structure in the COSMOS field is at the high end of the range of variations produced by sample variance (McCracken et al. 2007).

It is also instructive to plot the results in terms of differences with respect to one of the samples. For this exercise, the fiducial sample is set to the pure-parallel sample because the COSMOS field appears to be biased high. Figure 6 shows the resulting offsets in μ_0. Two trends are seen in the plot: (1) For all apertures, the COSMOS-field values of μ_0 are higher than the pure-parallel values in the range $21 \leq m \leq 23$, often at high significance, and (2) the lens fields often appear overdense compared to the pure-parallel fields, but the uncertainties on the lens values are so large that very few of the offsets are significantly different from zero. This result

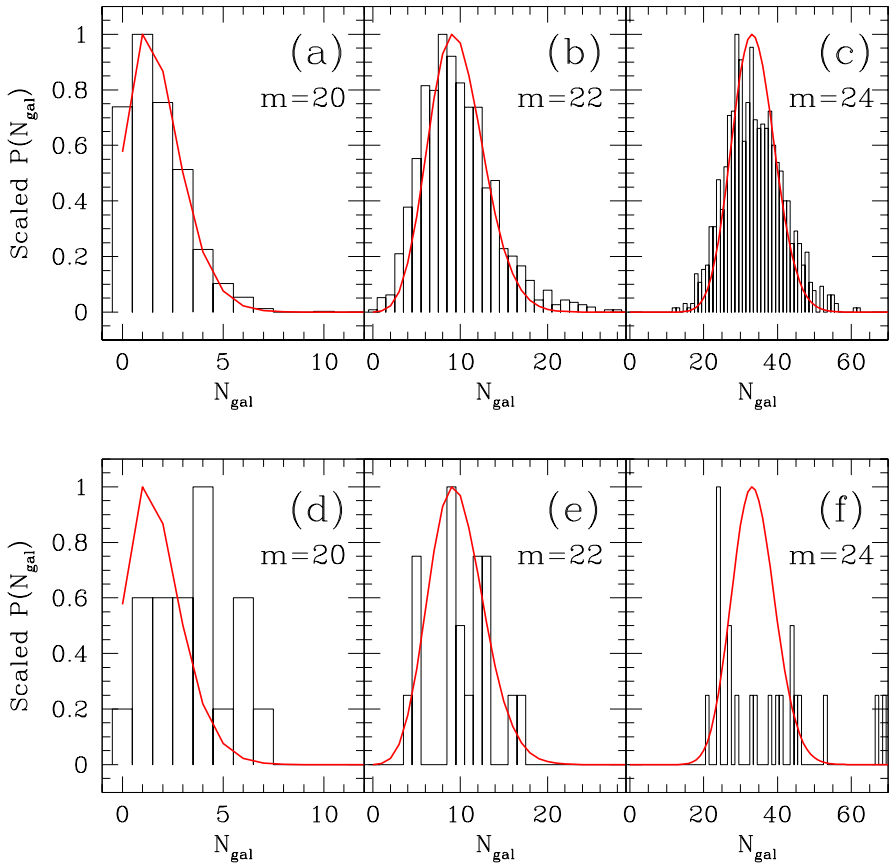

Figure 3. Histograms of number counts in the 45″aperture for two different samples: COSMOS (a–c) and lens fields (d–f). Shown are the magnitude bins $m = 20, 22, 24$ from right to left in each row. In both rows, the histograms represent the observed data while the solid curves represent a Poisson distribution with the same mean *as the COSMOS data.* Therefore, the Poisson distributions for the lens fields may not have the same means as the observed lens distributions. Whereas for bright galaxies the number-count variance can be explained by Poisson fluctuations, at fainter magnitudes (i.e. higher number counts; see panels *b* and *c*) the effect of sample variance becomes apparent.

is consistent with our frequentist analysis of the data (§3). Only for the smallest aperture (15.″9) do we see a significant trend for the lens fields, with the three bins at $m < 22$ all being $\geq 1\sigma$ higher than the pure parallel values. Clearly, a much larger lens sample is needed.

Overall, we can conclude that over a wide range of apertures ($\leq 45''$), the difference in the number of galaxies between lens and control field is less than ∼6 galaxies. Although this can be fractionally large, it clearly shows that on average only a few galaxies determine the difference between lens fields and non-lens fields in typical observations. For the smallest aperture of 15.″9, the difference is typically $\leq$ 1 galaxy at the 68% confidence level in any given magnitude bin. Since these galaxies have most influence on the lens model, taking these galaxies in to account has most impact on the lens model. We thus conclude that, given the uncertainties imposed by the size of our current lens samples, LSS variations do not make lens fields significantly overdense compared to non-lens fields. Only if mass does not follow light on average for the LSS could this conclusion be circumvented.

4.4 Correlation-function Corrections

In the previous subsection we saw that over the entire range of aperture sizes and magnitude limits, the average difference in the number of galaxies seen in the lens and control fields is typically $\lesssim 6$ for aperture sizes of 45″, integrated over all magnitudes (e.g., Fig. 6). Strangely, even though the pointings in both sets control fields are random (i.e. not centered on a bright galaxy), in the case of the COSMOS fields one often finds more galaxies than in the lens fields. This might be due to the fact that, unlike either the lens or pure-parallel fields, the COSMOS region is a contiguous field that may not be a representative sample of the Universe (i.e., it may be overdense).

Compared to the pure parallel fields, the lens fields are often slightly overdense, albeit at low significance. Based on the expectation values in Table 3, we calculate that the integrated (over magnitude) excess numbers of galaxies in the lens fields compared to the pure-parallel fields are 6.1 ± 3.7, 2.2 ± 3.8, 0.7 ± 2.8 and 2.9 ± 1.9, respectively, for the 45″, 31.″8, 22.″5 and 15.″9 apertures. This excess is not unexpected because the massive lens galaxies typically reside in *locally* overdense regions and, in principle, one would expect more galaxies in their neighborhood. To quantify the effect of local overdensities, we use the two-point correlation function

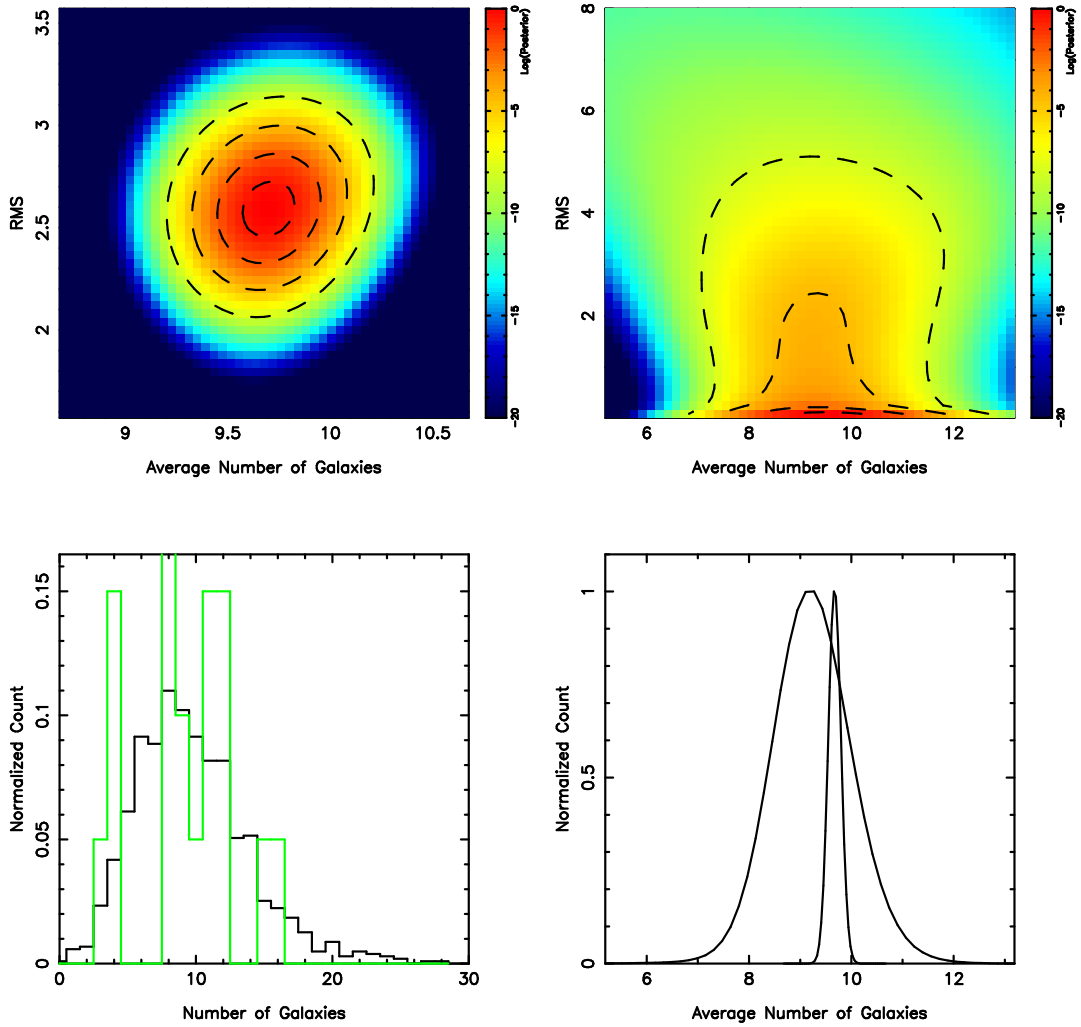

Figure 4. An illustration of the Bayesian derivation of the most likely average number of galaxies in the lens and control fields. Shown is the result for the largest (45″) aperture and $m = 22$ magnitude bin. Shown in the lower-left panel are the (normalized) number counts of lens (green) and control fields (black; COSMOS in this case) as function of the number of galaxies in those fields. The upper two panels show the likelihood of (μ_0, σ_0) for the lens (right) and control (left) fields, as determined from equation 4. The lower-right panel shows the marginalized probability function of μ_0 for the lens (broad function) and control (narrow function) fields. One notices from these curves that the most likely values of μ_0 for the lens and control field, in this illustration, are consistent.

of McCracken et al. (2007) and find predicted excesses (integrated over magnitude) of 2.0, 1.3, 0.9 and 0.6 galaxies, respectively, for the same apertures. After correcting for galaxy clustering, the difference between the lens and pure-parallel (or COSMOS) fields becomes insignificant, with differences only at the $\sim$1-σ level. We thus conclude that any line-of-sight overdensities in the lens fields, already being marginal, become insignificant when the local overdensities around the lens galaxies are accounted for.

To test the validity of the two-point correlation correction, we compared two sets of number counts derived from COSMOS. The first set is the one that we have used as the the first control sample, with number counts computed in grids of apertures placed on each COSMOS field. This set should be considered to represent "random" lines of sight through the COSMOS fields, since there is nothing special about the location of the aperture centers. In contrast, the apertures in the second set are each centered on a bright ($m < 20.5$) galaxy found in the COSMOS area. The bright-galaxy sample contains 1801 apertures. In Figure 7, we plot (1) the COSMOS "random" number counts, (2) the bright-galaxy number counts, and (3) the sum of the "random" number counts and the two-point correlation correction. The sum of the random number counts with the corrections from McCracken et al. (2007) are in excellent agreement with the number counts in apertures centered on bright galaxies.

Hence, *on average*, lines of sight to lens galaxies appear to be overdense only because of their local overdensities and not due to random structures along the lines of sight. Once these local overdensities, and any obvious clusters along the line of sight, have been included in the lens models, the determination of global values of cosmological parameters by averaging over lens samples should be unbiased.

5 COMMENTS ON INDIVIDUAL LENS SYSTEMS

Of course, the averages can hide quite a large variation from lens system to lens system. Fig. 8 shows the difference between the cumulative number counts of the lens sample and the COSMOS mean cumulative counts for the 45″ aperture. For the bright galaxies

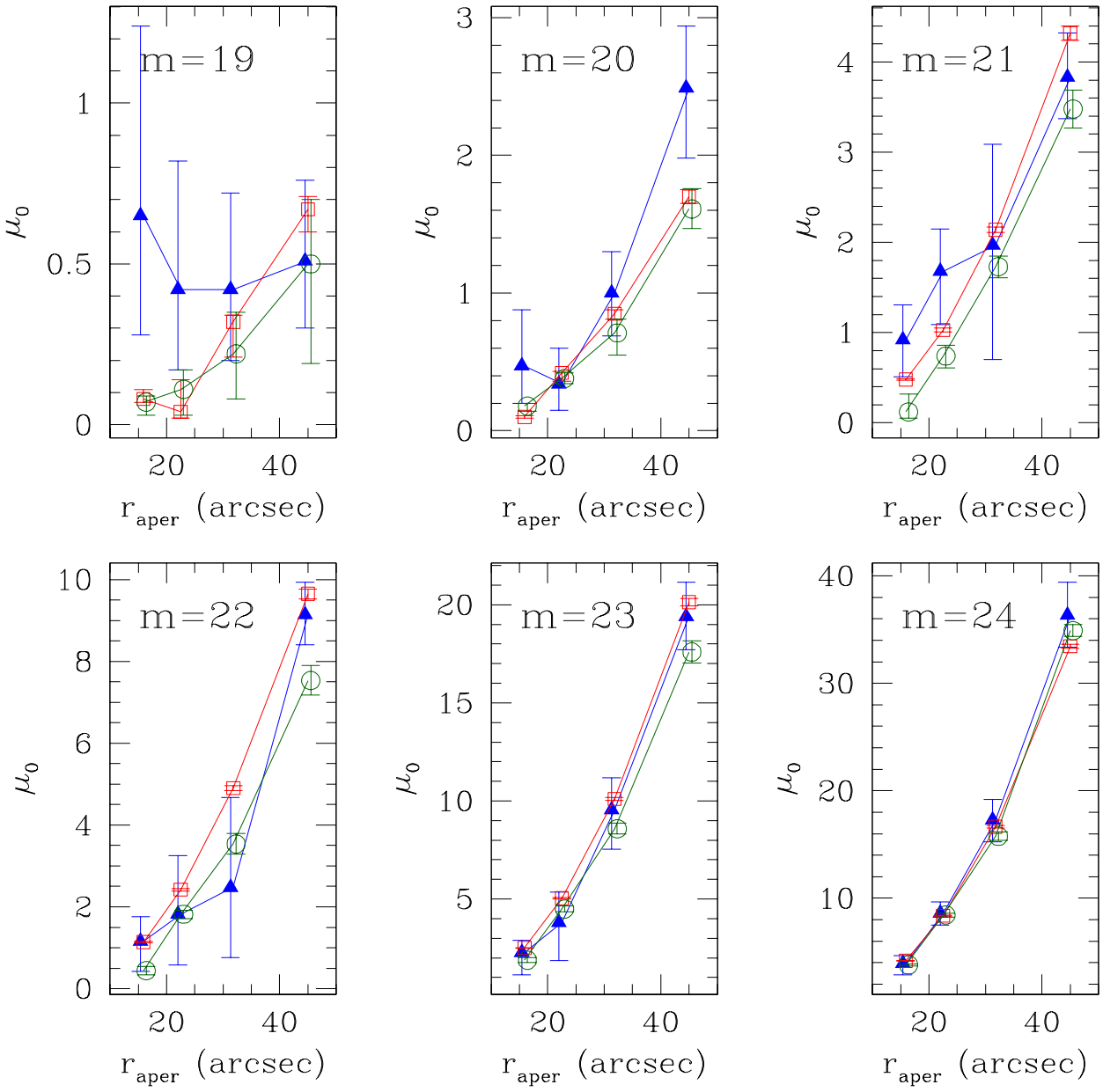

Figure 5. Plots of μ_0 vs. aperture size for each magnitude bin. In each plot, the blue triangles represent the lens sample, the red open squares represent the COSMOS sample, and the green open circles represent the pure-parallel sample. The value of μ_0 is determined for each aperture independently. Thus, for small numbers of galaxies, such as in the $m = 19$ bin, it is possible to have a larger fitted value of μ_0 in a smaller aperture than in the next larger aperture. Note that the COSMOS and pure-parallel points are formally inconsistent in several of the plots (e.g., m=21, 22, and 23).

($m \leq 22$), the lens fields with the largest overdensities are, in order starting with the most overdense, SDSS J1004+4112, B1608+656, and B2108+213. If considering all galaxies with $m \leq 24$, the three most overdense fields are SDSS J1004+4112, B1608+656, and B0218+357 (the three highest in Fig. 9). All of these fields are outside the region enclosing 90% of the COSMOS data. The overdensities for SDSS J1004+4112 and B2108+213 are not particularly surprising because each of these systems is known to be associated with a cluster or rich group (Oguri et al. 2004; McKean et al. 2009). However, neither B1608+656 nor B0218+357 appear to be physically associated with such massive concentrations of galaxies. Spectroscopic observations of the B1608+656 field have revealed multiple group-sized associations along the line of sight (Fassnacht et al. 2006b), but the B0218+357 field will have to be examined more closely in future analyses. Because B0218+357 (Biggs et al. 1999), SDSS J1004+4112 (Fohlmeister et al. 2007, 2008), and B1608+656 (Fassnacht et al. 1999, 2002) are systems for which time delays have been measured, these overdensities with respect to the mean line of sight must be included in any analysis to determine H_0 from these systems. Fig. 8 also reveals fields

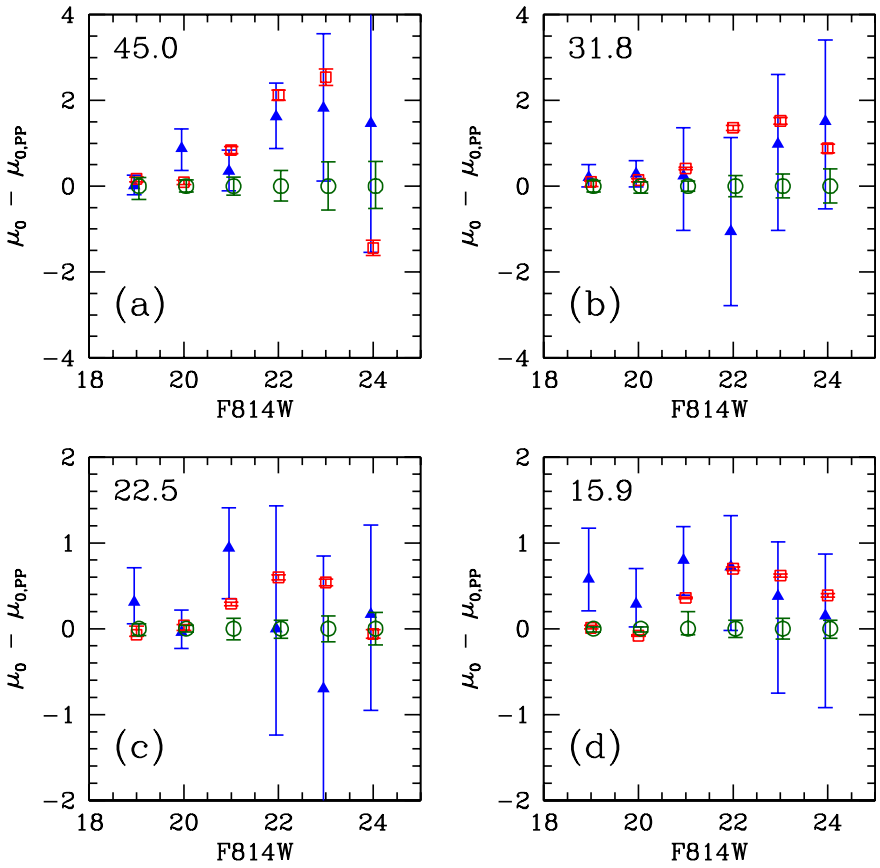

Figure 6. Results of Bayesian analysis, showing the *difference* between the values of μ_0 calculated for the pure parallel fields (green circles) and those obtained for the lens (blue triangles) and COSMOS fields (red squares) fields. Note the significant displacement between the pure parallel fields and the COSMOS fields, particularly for $21 \leq m < 23$.

that are underdense with respect to the mean. The most underdense in bright galaxies are SDSS 1226−0006, J0816+5003, and B0850+054. Although time delays have not yet been measured for any of these systems, similar care should be taken in future H_0 analyses that are based on the lens systems individually.

6 INTERPRETATION & CONCLUSIONS

To assess whether strong gravitational lenses are preferentially found along overdense lines of sight, we have devised a straightforward Bayesian statistical number-count test which is conservative and robust. It requires only the number counts of galaxies as function of magnitude inside apertures of different sizes centered on the lenses and on control fields. We have applied this method to a sample 20 lenses with F814W ACS images and control samples from the COSMOS and pure-parallel programs.

Our hypothesis is that *if* gravitational lenses are found along highly overdense lines of sight compared to random pointings on the sky, either due to structure along the line of sight or overdensities associated with the lens galaxies themselves, *then* the number of galaxies within apertures centered on the lenses should show on average more galaxies than similar apertures in the control fields. This approach is conservative in that it does not require redshifts for the galaxies (hence for a given magnitude, galaxies over a wide redshift range contribute to the number counts), but only that the ratio between mass and light integrated over the redshift cone is close to constant. Thus, the number of galaxies can be used as a proxy for mass; more galaxies on average implies more mass along the line of sight.

More precise statistics can be constructed if the redshifts, galaxy types, etc. are known, and the galaxy masses are derived through scaling relations such as the Tully-Fisher relation (Tully & Fisher 1977) or the fundamental plane (Djorgovski & Davis 1987; Dressler et al. 1987). However, the results of such models quickly become model-dependent and prone to systematic errors. Thus, although such approaches may show a more significant result than ours, a rejection of the hypothesis by our approach has the advantage of being a robust result that is less dependent on model assumptions.

Having applied our number-count comparison to the selected lens and control fields we find the following results:

(i) All distribution functions of number counts in the lens and

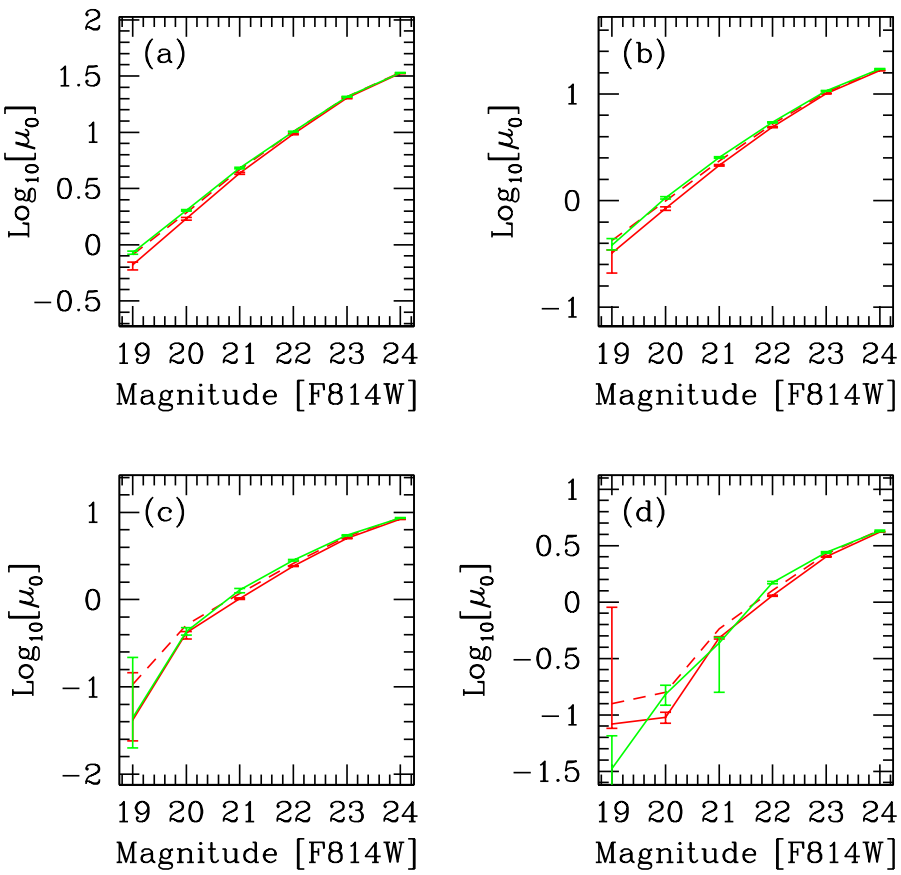

Figure 7. Comparison of number counts between the COSMOS control sample (red) and apertures centered on bright galaxies in COSMOS (green). The dashed line represents the sum of the control sample number counts and the two-point correlation correction factors.

control fields are well described by a combination of a Gaussian random field for the sample variance (i.e., the underlying density field varies from field to field) and Poisson statistics in the number counts. This defines our underlying Bayesian statistical model.

(ii) In the three largest apertures, with radii of $45''$, $38\farcs1$ and $22\farcs5$ (steps of 2 in area), we find *no* significant difference in the number counts between the lens and control fields (Fig. 6 and Table 3). We emphasize that this does not presuppose that there is no overdensity, just that our robust statistics do not require it. We do see a mildly significant overdensity in the $m = 19$ bin in the $22\farcs5$ aperture, which might hint that indeed there are more bright galaxies near the lines of sight to lens galaxies.

(iii) The smallest aperture ($15\farcs9$) centered on the lenses, however, does show significantly more galaxies in the magnitude range $m = 19 - 21$ than either the COSMOS or pure parallel fields. This is not unexpected since massive lens galaxies live in overdense regions (their two-point correlation is strong).

(iv) When we correct for the effect of the two-point correlation, using the results from COSMOS by McCracken et al. (2007), we find that a significant part of the differences between number counts in the lens and COSMOS fields can be accounted for by the fact that massive lens galaxies live in *locally* overdense regions, as expected. The remaining differences lie within the ~ 1–σ errors on the number counts, even though the lens fields still show slightly higher number counts in the range $19 \leq m \leq 21$ in the smallest aperture. These differences could either be due to small overdensities along the line of sight (e.g., Fassnacht & Lubin 2002; Momcheva et al. 2006; Fassnacht et al. 2006b; Auger et al. 2007), or due to a too simplistic correction of the number counts for the COSMOS two-point correlation function.

(v) On average, the excess numbers of galaxies along the lines of sight to the lensing galaxies, integrated over the magnitude range that we have explored in this paper, are small (e.g., $\lesssim 6$ galaxies for the largest aperture that we examined). These excesses, which are mainly due to local overdensities associated with the lensing galaxy, amount to only $\sim$4–8% of the total number counts in the three largest apertures. These fractional overdensities can be compared with similar numbers derived from numerical simulations. In particular, Hilbert et al. (2007) found, by ray tracing through the Millennium Simulation (Springel et al. 2005), that lenses do along biased lines of sight. The contribution of the additional mass, however, was only a few percent of the total surface mass density along those lines of sight, in good agreement with our results.

(vi) While the average number counts in our sample of 20 strong lenses does agree well with the control samples, once the effect of local clustering has been taken out, individual lens systems can still

Table 3. Estimated value of the mean underlying number counts μ_0 in the lens, COSMOS, and pure-parallel fields.

Radius (Arcsec.)	m (mag.)	Lens	COSMOS	Pure-parallel
45.0	19	$0.51^{+0.25}_{-0.21}$	$0.67^{+0.04}_{-0.07}$	$0.50^{+0.20}_{-0.31}$
	20	$2.49^{+0.45}_{-0.51}$	$1.70^{+0.05}_{-0.05}$	$1.61^{+0.15}_{-0.14}$
	21	$3.83^{+0.49}_{-0.46}$	$4.32^{+0.08}_{-0.08}$	$3.48^{+0.21}_{-0.21}$
	22	$9.15^{+0.78}_{-0.74}$	$9.65^{+0.12}_{-0.12}$	$7.53^{+0.37}_{-0.35}$
	23	$19.41^{+1.73}_{-1.70}$	$20.13^{+0.19}_{-0.19}$	$17.59^{+0.57}_{-0.56}$
	24	$36.36^{+3.03}_{-3.00}$	$33.46^{+0.18}_{-0.18}$	$34.90^{+0.58}_{-0.52}$
31.8	19	$0.42^{+0.30}_{-0.22}$	$0.32^{+0.02}_{-0.11}$	$0.22^{+0.13}_{-0.14}$
	20	$1.00^{+0.30}_{-0.31}$	$0.85^{+0.03}_{-0.04}$	$0.71^{+0.10}_{-0.16}$
	21	$1.97^{+1.12}_{-1.27}$	$2.14^{+0.03}_{-0.03}$	$1.73^{+0.12}_{-0.12}$
	22	$2.48^{+2.19}_{-1.72}$	$4.90^{+0.06}_{-0.06}$	$3.54^{+0.25}_{-0.25}$
	23	$9.56^{+1.62}_{-2.01}$	$10.10^{+0.08}_{-0.08}$	$8.58^{+0.28}_{-0.27}$
	24	$17.27^{+1.90}_{-2.04}$	$16.64^{+0.10}_{-0.10}$	$15.76^{+0.40}_{-0.39}$
22.5	19	$0.42^{+0.40}_{-0.25}$	$0.04^{+0.10}_{-0.02}$	$0.11^{+0.06}_{-0.08}$
	20	$0.34^{+0.26}_{-0.19}$	$0.42^{+0.01}_{-0.06}$	$0.38^{+0.04}_{-0.04}$
	21	$1.68^{+0.47}_{-0.59}$	$1.03^{+0.02}_{-0.02}$	$0.74^{+0.12}_{-0.13}$
	22	$1.82^{+1.43}_{-1.24}$	$2.42^{+0.03}_{-0.03}$	$1.82^{+0.10}_{-0.11}$
	23	$3.80^{+1.55}_{-1.93}$	$5.04^{+0.04}_{-0.04}$	$4.50^{+0.15}_{-0.15}$
	24	$8.60^{+1.04}_{-1.12}$	$8.37^{+0.05}_{-0.05}$	$8.43^{+0.19}_{-0.19}$
15.9	19	$0.65^{+0.59}_{-0.37}$	$0.08^{+0.01}_{-0.01}$	$0.07^{+0.02}_{-0.04}$
	20	$0.47^{+0.41}_{-0.27}$	$0.10^{+0.01}_{-0.01}$	$0.18^{+0.02}_{-0.04}$
	21	$0.92^{+0.39}_{-0.41}$	$0.48^{+0.01}_{-0.01}$	$0.12^{+0.20}_{-0.07}$
	22	$1.16^{+0.60}_{-0.74}$	$1.14^{+0.02}_{-0.02}$	$0.44^{+0.10}_{-0.10}$
	23	$2.27^{+0.63}_{-1.13}$	$2.51^{+0.02}_{-0.02}$	$1.89^{+0.12}_{-0.12}$
	24	$3.94^{+0.72}_{-1.07}$	$4.18^{+0.02}_{-0.02}$	$3.79^{+0.10}_{-0.11}$

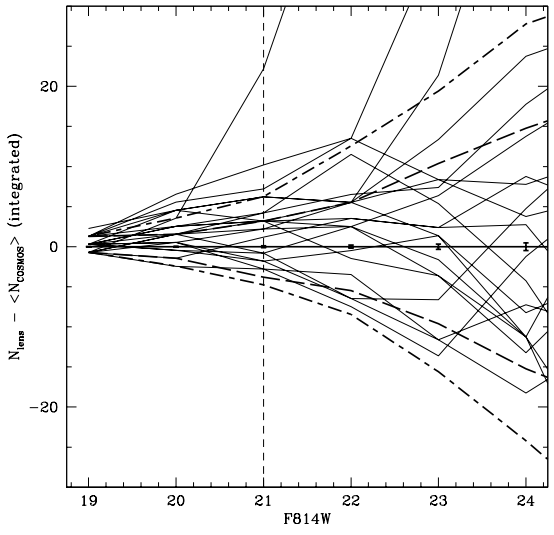

Figure 8. Difference between lens sample cumulative number counts (light lines) and the COSMOS mean cumulative number counts (heavy solid line) with apertures of radius $45''$. The heavy dashed and dot-dashed lines represent the 68% and 90% ranges, respectively, of the COSMOS number counts. The light dashed vertical line is placed solely to identify the three most overdense lens fields. Starting at the top of the figure and going down, the line encounters, in order, the curves for SDSS J1004+4112, B1608+656, and B2108+213, all of which fall outside the 90% range of COSMOS field number counts.

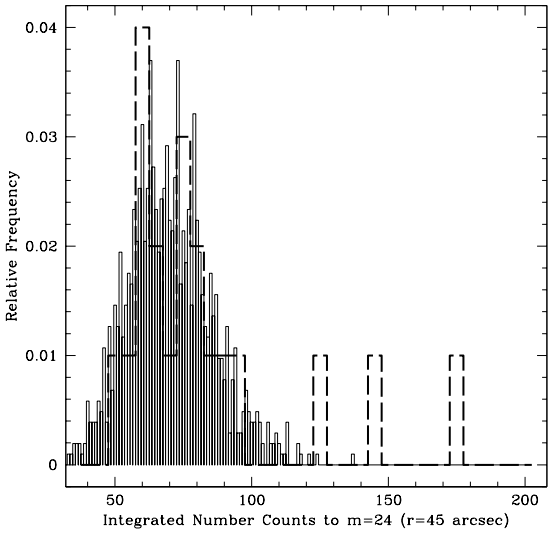

Figure 9. Distribution of number counts in the COSMOS (light solid lines) and lens (heavy dashed line) fields. Plotted are the integrated number counts for all galaxies with $m \leq 24$ inside $45''$ apertures

have significantly discrepant number counts. Thus, care should be taken when using an individual lens system to measure H_0.

Based on our statistical test, we can say that: Yes, lens galaxies live along overdense lines of sight compared to random pointings on the sky, but these overdensities can be nearly fully explained by the fact that these massive lens galaxies are formed in locally overdense regions. The contribution by everything else along the line of sight is, in our test, not significant on average.

Overall, we conclude that in strong-gravitational lens modeling one always needs to assess the effect of the *local* overdense field, but that the effect of the uncorrelated line-of-sight over- and underdensities should average out in large samples (at least $\gtrsim 20$ as in our case). As an example, we therefore expect the *global* value of H_0 from lensing to be little affected by line-of-sight effects, but it could become biased if the local overdensities of the fields in which the lenses are embedded are not accounted for in the modeling.

We thank Phil Marshall and Tommaso Treu for fruitful discussions. We thank Phil Marshall and Tim Schrabback for their work on the HAGGLeS pipeline and their help in modifying the pipeline to run on the pure-parallel data. CDF acknowledges support under HST program #AR-10300, which was provided by NASA through a grant from the Space Telescope Science Institute, which is operated by the Association of Universities for Research in Astronomy, Inc., under NASA contract NAS 5-26555. He is also grateful for the generous hospitality shown by the Kapteyn Institute on his visits there. LVEK is supported (in part) through an NWO-VIDI program subsidy (project number 639.042.505). This work is supported by the European Community's Sixth Framework Marie Curie Research Training Network Programme, Contract No. MRTN-CT-2004-505183 'ANGLES'.

REFERENCES

Auger M. W., Fassnacht C. D., Wong K. C., Thompson D., Matthews K., Soifer B. T., 2008, ApJ, 673, 778

Auger M. W., 2008, MNRAS, 383, L40
Auger M. W., Fassnacht C. D., Abrahamse A. L., Lubin L. M., Squires G. K., 2007, AJ, 134, 668
Bardeen, J. M., Bond, J. R., Kaiser, N., & Szalay, A. S. 1986, ApJ, 304, 15
Bar-Kana, R. 1996, ApJ,468, 17
Bertin, E. & Arnouts, S. 1996, A&A, 117, 393
Biggs A. D., Browne I. W. A., Helbig P., Koopmans L. V. E., Wilkinson P. N., Perley R. A., 1999, MNRAS, 304, 349
Djorgovski S., Davis M., 1987, ApJ, 313, 59
Dressler A., 1980, ApJ, 236, 351
Dressler A., Lynden-Bell D., Burstein D., Davies R. L., Faber S. M., Terlevich R., Wegner G., 1987, ApJ, 313, 42
Falco, E. E., Gorenstein, M. V., & Shapiro, I. I. 1985, ApJL, 289, L1
Fassnacht, C. D. & Lubin, L. M. 2002, AJ, 123, 627
Fassnacht C. D., Pearson T. J., Readhead A. C. S., Browne I. W. A., Koopmans L. V. E., Myers S. T., Wilkinson P. N., 1999, ApJ, 527, 498
Fassnacht C. D., Xanthopoulos E., Koopmans L. V. E., Rusin D., 2002, ApJ, 581, 823
Fassnacht C. D., et al., 2006, ApJ, 651, 667
Fassnacht C. D., Gal R. R., Lubin L. M., McKean J. P., Squires G. K., Readhead A. C. S., 2006, ApJ, 642, 30
Faure C., et al., 2009, ApJ, 695, 1233
Fohlmeister J., et al., 2007, ApJ, 662, 62
Fohlmeister J., Kochanek C. S., Falco E. E., Morgan C. W., Wambsganss J., 2008, ApJ, 676, 761
Ford, H., et al. 1998, Proc. SPIE, 3356, 234
Ford, H., et al. 2002, Proc. SPIE, 4854, 81
Gregory, P. C. 2005, Bayesian Logical Data Analysis for the Physical Sciences: A Comparative Approach with 'Mathematica' Support. Edited by P. C. Gregory. ISBN 0 521 84150 X Published by Cambridge University Press, Cambridge, UK, 2005
Hilbert S., White S. D. M., Hartlap J., Schneider P., 2007, MNRAS, 382, 121
Hilbert S., White S. D. M., Hartlap J., Schneider P., 2008, MNRAS, 386, 1845
Keeton, C. R., & Zabludoff, A. I. 2004, ApJ, 612, 660
Koekemoer, A. M., Fruchter, A. S., Hook, R., & Hack, W. 2002, in *2002 HST Calibration Workshop*, eds. S. Arribas, A. Koekemoer, & B. Whitmore. Baltimore, MD: Space Telescope Science Institute, 2002., p.339
Koekemoer, A. M., et al. 2007, ApJS, 172, 196
Kundić T., Cohen J. G., Blandford R. D., Lubin L. M., 1997, AJ, 114, 507
Kundić T., Hogg D. W., Blandford R. D., Cohen J. G., Lubin L. M., Larkin J. E., 1997, AJ, 114, 2276
Leauthaud A., et al., 2007, ApJS, 172, 219
Massey R., et al., 2007, ApJS, 172, 239
McCracken, H. J., et al., 2007, ApJS, 172, 314
McKean, J. P., Auger, M. W., Koopmans, L. V. E., Vegetti, S., Czoske, O., Fassnacht, C. D., Treu, T., More, A., & Kocevski, D. D., 2009, MNRAS, submitted
Momcheva I., Williams K., Keeton C., Zabludoff A., 2006, ApJ, 641, 169
Oguri M., et al., 2004, ApJ, 605, 78
Schneider P., Kochanek C. S., Wambsganss J., 2006, Gravitational Lensing: Strong, Weak and Micro: Saas-Fee Advanced Courses, Volume 33. Springer-Verlag, Berlin, Heidelberg
Scoville, N., et al. 2007, ApJS, 172, 1
Scoville, N., et al. 2007, ApJS, 172, 38
Seljak, U. 1994, ApJ, 436, 509
Springel V., et al., 2005, Nature, 435, 629
Treu T., Gavazzi R., Gorecki A., Marshall P. J., Koopmans L. V. E., Bolton A. S., Moustakas L. A., Burles S., 2009, ApJ, 690, 670
Tully R. B., Fisher J. R., 1977, A&A, 54, 661
Wambsganss J., Bode P., Ostriker J. P., 2005, ApJ, 635, L1
Williams K. A., Momcheva I., Keeton C. R., Zabludoff A. I., Lehár J., 2006, ApJ, 646, 85
Zabludoff A. I., Mulchaey J. S., 1998, ApJ, 496, 39